

27p.

N62-16382

Technical Report No. 32-346

*Simplified Free-Flight Testing in a
Conventional Wind Tunnel*

Bain Dayman, Jr.

		OTS PRICE
XEROX	\$	<u>2.60 ph</u>
MICROFILM	\$	<u>1.01 mf</u>



**JET PROPULSION LABORATORY
CALIFORNIA INSTITUTE OF TECHNOLOGY
PASADENA, CALIFORNIA**

October 1, 1962

NATIONAL AERONAUTICS AND SPACE ADMINISTRATION
CONTRACT NO. NAS 7-100

Technical Report No. 32-346

*Simplified Free-Flight Testing in a
Conventional Wind Tunnel*

Bain Dayman, Jr.

Robert E. Covey

Robert E. Covey, Chief
Aerodynamic Facilities Section

JET PROPULSION LABORATORY
CALIFORNIA INSTITUTE OF TECHNOLOGY
PASADENA, CALIFORNIA

October 1, 1962

Copyright© 1962
Jet Propulsion Laboratory
California Institute of Technology

CONTENTS

I. Introduction	1
II. Approximate Equations of Motion	2
III. Model Design and Construction	3
IV. Model Release Technique	5
V. Data Acquisition	6
VI. Sphere Drag	7
VII. Free-Flight Sphere Wakes	10
VIII. Effect of Vertical Wire Support on Sphere Wakes	11
IX. Aerodynamic-Shape Free-Flight Data	11
X. Summary of Some Advantages of Free-Flight Testing in a Wind Tunnel	16
XI. Additional Comments	18
XII. Future Work	19
XIII. Conclusions	20
Nomenclature	21
References	22
Table I. Analytical estimate of cone drag (20-deg half angle)	16

FIGURES

1. The ratio $r_s m/I$ vs. r_c/r_s for a spherical model	3
2. Photographs of typical test models	4
3. Photograph of test installation	5
4. Example of 35-mm half-frame motion pictures taken at 4000 frames/sec	6
5. Pictures showing travel of sphere model across viewing window	8
6. Model-position history of free-flight sphere	9

FIGURES (Cont'd)

7. Velocity history of free-flight sphere	9
8. Spark schlieren pictures of sphere wakes	10
9. Aerodynamic-shape model dimensions	11
10. Composite picture of aerodynamic shape in flight	12
11. Model-position history of aerodynamic shape	13
12. Velocity history of aerodynamic-shape model	13
13. Composite pictures of aerodynamic shapes in flight	14
14. Free-flight spark schlieren picture of aerodynamic-shape model	15

ACKNOWLEDGMENT

By the very nature of this testing technique, its success is dependent upon the efforts of the various technical groups involved. Their imagination and patient approach to the problems of model construction, model release, photography, and test conduction were the primary factors for the early success of this free-flight testing technique.

ABSTRACT

16382

In order to incorporate the advantages of ballistic range testing with the convenience of wind tunnel testing, simplified techniques have been developed at the Jet Propulsion Laboratory (JPL) for free-flight testing of models in a conventional wind tunnel. So far, only a small number of the many possibilities have been investigated, but the preliminary results indicate that such techniques are both practical and useful. The model to be investigated is suspended on a single traverse wire at the upstream end of the test section window, then is released from this position by causing the wire to break within the model. High speed motion pictures taken of the model oscillating during its travel across the viewing area make it possible to determine various aerodynamic parameters such as drag, lift, pitching moment, and pitch damping in much the same manner as is done in ballistic range testing. Also, a spark schlieren photograph can be taken of the model in flight in order to observe details of an undisturbed (from support interference) wake.

I. INTRODUCTION

The ability to obtain aerodynamic data on models without interference from a model support system is a desired and sometimes necessary testing technique. The supportless manner of testing is one important feature of the ballistic range. Free-flight testing of models has been done quite successfully in shock tunnels (Refs. 1, 2) and has been attempted in "hot-shot" intermittent facilities (Ref. 3). In these tunnels the model is suspended in the test section on very fine wires which are broken during the flow starting process, thereby releasing the model into a free-flight trajectory through the test section. This wire support procedure was adapted for use in the continuous-flow wind tunnels at JPL with the added control of being able to release the model upon demand after flow has been established.

Aerodynamic force and moment data are normally obtained in a conventional wind tunnel by supporting the model on a sting and measuring the resulting air loads

with a balance. In some cases the aft portion of the model must be altered in order to accommodate an internal balance or a sting. This alteration does have effect upon the aerodynamic loads and must be investigated in order to establish the magnitude of the effects. Also affecting aerodynamic loads is the presence of most supports (such as wires, side-mount thin wings, or rear stings) which alter the flow from that which would exist in the absence of any support.

This report will discuss the few experiments that have already been performed, what work is being contemplated for the very near future, and some advantages of incorporating free-flight testing as another standard testing technique in a conventional wind tunnel.*

*The data appearing in this report (unless otherwise stated) are from a series of tests conducted in the JPL 20-in. Supersonic Wind Tunnel during April and May, 1962.

II. APPROXIMATE EQUATIONS OF MOTION

In order to design the models for a free-flight run it is first necessary to determine the expected motion of the model. The model motion across the schlieren-system viewing window can be approximated by assuming that the dynamic pressure [$\frac{1}{2}\rho(V_\infty - V_m)^2$] acting upon the model is constant, i.e., $V_m = 0$. As the ratio V_m/V_∞ may be as large as 5% (resulting in a dynamic pressure degradation of some 10%) the final reduced data must account for this variation. However, for $V_m/V_\infty < 0.1$ the assumption of freestream dynamic pressure acting upon the model during its flight across the viewing window is adequate for model design.

The simplified linear solution to the usual captive-model wind tunnel dynamic stability-in-pitch equation is:

$$I\ddot{\alpha} + M_D\dot{\alpha} + M_\alpha\alpha = 0$$

This gives the approximate relations for the frequency and the decay in the amplitude of oscillation of:

$$f = \frac{1}{2\pi} \left(\frac{M_\alpha}{I} \right)^{\frac{1}{2}}$$

$$\frac{\alpha_t}{\alpha_0} = \exp \left(- \frac{M_D}{2I} t \right)$$

These solutions, in conjunction with the force equals mass times acceleration relationship, yield the following equations which are useful in designing models for free-flight testing in the wind tunnel:

- (1) Model acceleration:

$$a = \frac{q_\infty C_D A}{W} g$$

- (2) Time to travel distance S:

$$t = \left(\frac{2Sm}{q_\infty C_D A} \right)^{\frac{1}{2}}$$

- (3) Model velocity at distance S:

$$V_m = \left(\frac{2Sq_\infty C_D A}{m} \right)^{\frac{1}{2}}$$

- (4) Number of complete oscillation cycles in distance S:

$$N = \frac{1}{\pi} \left(\frac{C_{m_\alpha}}{C_D} S \frac{d}{2} \frac{m}{I} \right)^{\frac{1}{2}}$$

- (5) Oscillation frequency:

$$f = \frac{1}{2\pi} \left(\frac{C_{m_\alpha} A d q_\infty}{I} \right)^{\frac{1}{2}}$$

- (6) Decay in amplitude of oscillation:

$$\frac{\alpha_t}{\alpha_0} = \exp \left(- \frac{M_D}{2I} t \right)$$

where

$$M_D = (C_{m_q} + C_{m_{\dot{\alpha}}}) q_\infty A \frac{d^2}{V_\infty}$$

III. MODEL DESIGN AND CONSTRUCTION

The choice of model size, materials, and mode of construction is dependent upon the data desired at the chosen wind-tunnel flow conditions. For drag measurements the design is based merely on the acceleration compatible for the frame-rate of the high-speed motion picture camera with the consideration that too low an acceleration (below 20 g) will allow the model to drop too far during its travel across the viewing area. Of course, the model center of gravity must be sufficiently forward of the center of pressure to ensure model stability.

The model design is somewhat complicated when pitch-moment data are desired. As can be seen from the approximate equations of motion, the number of oscillation cycles during the model's travel across the viewing area is a function (among other things) of the model size and the ratio of the model mass to the moment of inertia about its center of gravity. For similarly constructed models, the number of oscillation cycles is proportional to the inverse square root of the model size, resulting in an increase in the number of oscillation cycles with a decrease in model size. Also, in order to increase the ratio of mass to moment of inertia, the model shape can be a thin shell or else a very lightweight solid materials (such as 2 lb/ft³ polyurethane foam) with a spherical core of lead or, preferably, gold. The size of the core can be chosen to optimize the ratio m/I . For purposes of demonstration, Fig. 1 shows the variation of the value $r_s(m/I)$ with r_c/r_s for various diameters of spherical models (1/2- to 3-in. diam) made out of a heavy core (such as lead or gold) at the center of a light-weight substance, perhaps polyurethane foam, such that the density of the core is 100 or 200 times the density of the homogeneous outer shell. Usually it is desirable to choose a ratio of r_c/r_s on the high side to increase the model weight and thus decrease the model acceleration.

For the series of tests discussed in this Report the test spheres were made of silastic rubber with powdered lead added to give the desired densities (varying from a specific gravity of 1.1 with no lead added, to 3.4 with the maximum amount of lead added). The aerodynamic-shape models were made from a 2 lb/ft³ polyurethane foam mixture which yielded an average density of 6 lbs/ft³ when molded. Then a 0.45-in. diam spherical lead core was added slightly forward of the desired model center of gravity location. Several typical models are shown in Fig. 2.

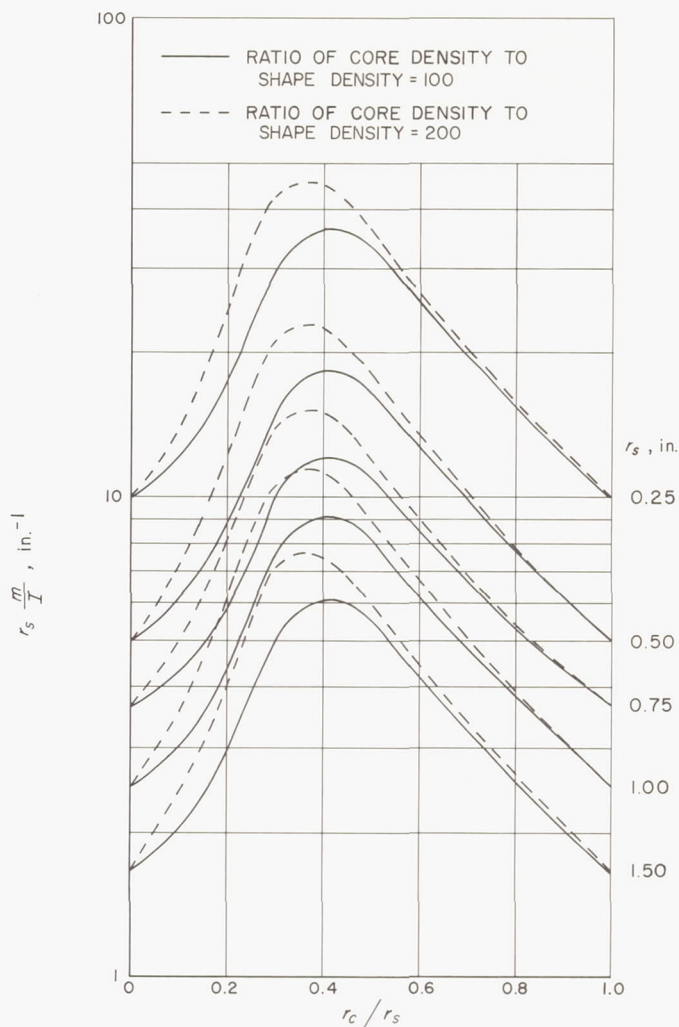
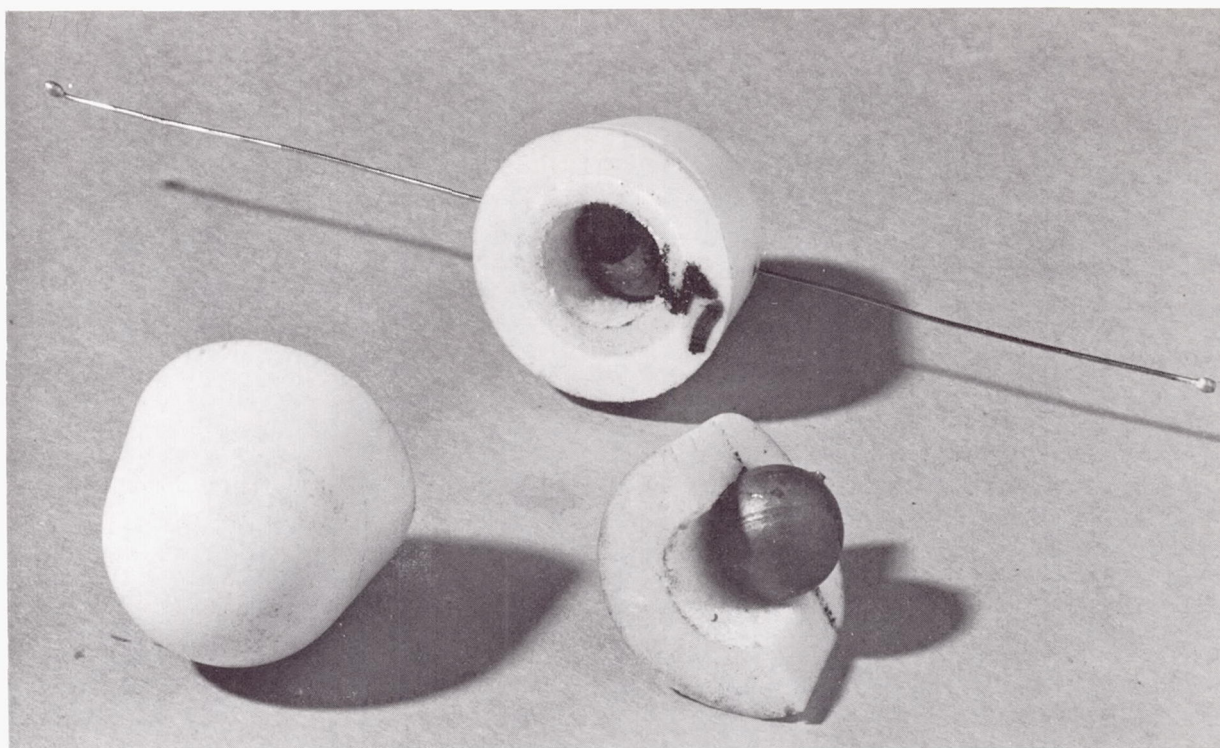


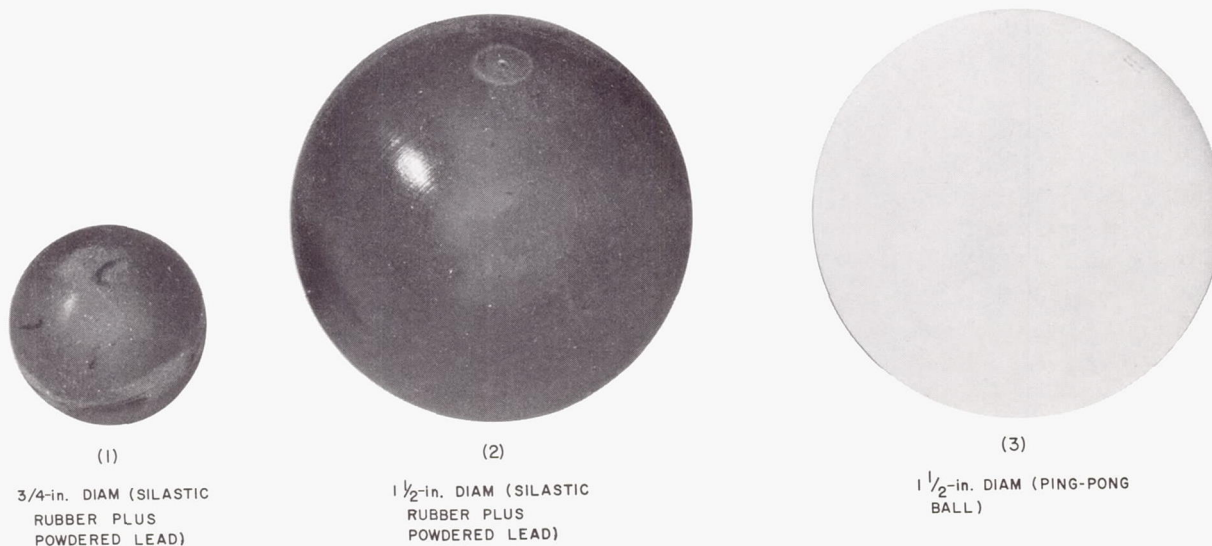
Fig. 1. The ratio $r_s m/I$ vs. r_c/r_s for a spherical model

As the maximum accelerations experienced by the models prior to and during the data acquisition period are usually below $10^2 g$, the models can be of very delicate, yet simple, construction. For example, the center of gravity can be located far forward in the model. Also, airplane models having "flimsy" surfaces can be easily built and successfully tested. Adequate construction of the *Apollo* abort configuration (re-entry capsule and tower with rocket) presents very little difficulty even though the tower design consists of a fine skeletal framework. These few examples serve to illustrate the many possible advantages for model construction due to the relatively low loads that models experience during free-flight testing in a wind tunnel.



A. AERODYNAMIC SHAPE

LENGTH = 0.825 in.
BASE-DIAM = 1 in.
LEAD-CORE DIAM = 0.45 in.
SUPPORT-WIRE DIAM = 0.020 in.



(1)
3/4-in. DIAM (SILASTIC
RUBBER PLUS
POWDERED LEAD)

(2)
1 1/2-in. DIAM (SILASTIC
RUBBER PLUS
POWDERED LEAD)

(3)
1 1/2-in. DIAM (PING-PONG
BALL)

B. SPHERES

Fig. 2. Photographs of typical test models

IV. MODEL RELEASE TECHNIQUE

In general, each model was supported at the upstream edge of the test section window on a vertical 0.020-in. diam wire which was notched, within the model, to a depth of 0.005 in. This wire was preloaded with a seventy pound tension. The installation is shown in Fig. 3. An impulse load of 10 lb would cause the wire to break at the notch, releasing the model for its flight across the tunnel viewing area. The wire pulling out of the models seldom imparted any vertical or oscillatory motion to the models. In order to support the models on a horizontal "wire," a 0.040-in. diam monofilament string was used. (Because the wires are blown back against the test section walls upon being broken, string must be used in place of wire for the horizontal support in order to prevent damage to the viewing windows.) It was knotted inside the model in order to create a stress point so that when an impulse load was added to the tension load a break would occur within the model. The vertical wire technique was very dependable, but the horizontal string technique requires more development as it was not successful all of the time. With either technique, 2 or 3 "flights" per hour were achieved.

The spheres as well as the aerodynamic-shape models at zero angle of attack were supported on the vertical wire. In order to give aerodynamic-shape models an initial angle of attack so as to cause them to oscillate during their travel, it is necessary to support them on:

- (1) A horizontal string which passes through the model away from the center of gravity in order that the model is free to weathervane in a plane parallel to the viewing-window surface. The models are stable prior to release.
- (2) A vertical wire which passes through the model center of gravity but at an angle to the base equal to the desired angle of attack prior to the release. This technique also causes the model to oscillate in a plane parallel to the viewing window surface. However, some models may be unstable prior to release and consequently will "buzz."
- (3) A vertical wire which passes through the model away from the center of gravity in order that the model is free to weathervane in a plane perpen-

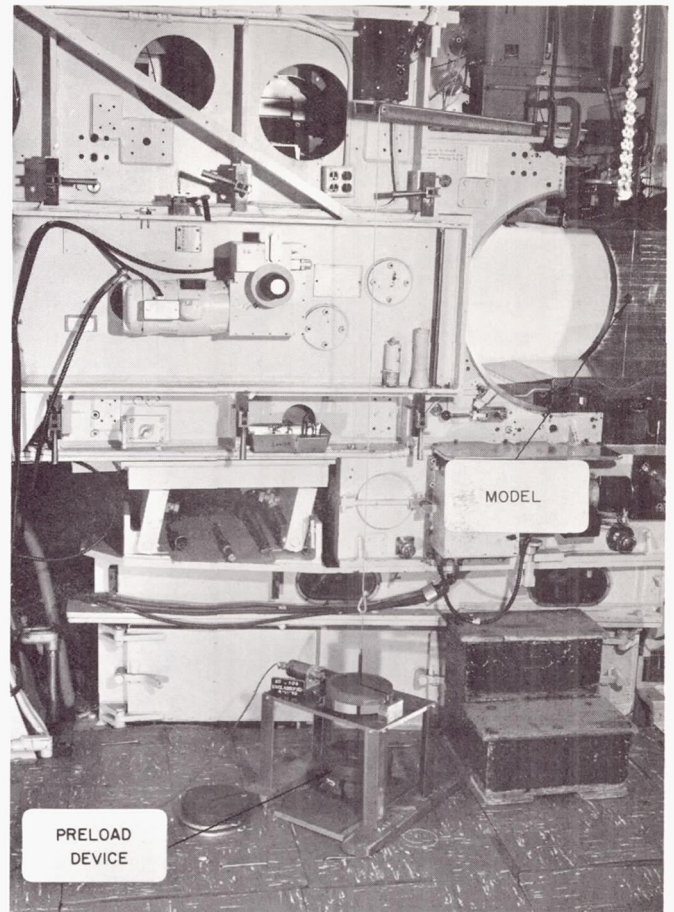


Fig. 3. Photograph of test installation

dicular to the viewing-window surface. The models are stable prior to release. Although the model oscillations are generally confined to this perpendicular plane and the period of oscillation can be quite accurately determined, the amplitude of oscillation can only be estimated.

With the use of a single wire support, not only can the magnitude of the model's angle-of-attack oscillation amplitude be easily and accurately controlled, but large amplitudes are practical such as were obtained for the aerodynamic-shape runs ($\alpha \approx 40$ deg) discussed in this Report.

V. DATA ACQUISITION

Two types of free-flight data were obtained. In order to obtain fairly detailed information on the wake shapes, normal wind-tunnel spark schlierens were obtained for each model at one point of its trajectory. For this type of data the models were supported in order to give zero angle of attack during the flights. For less detailed pictures of the model wakes, high-speed (4000 frames/sec) motion picture schlierens were taken. This technique is useful for wake studies of oscillating models.

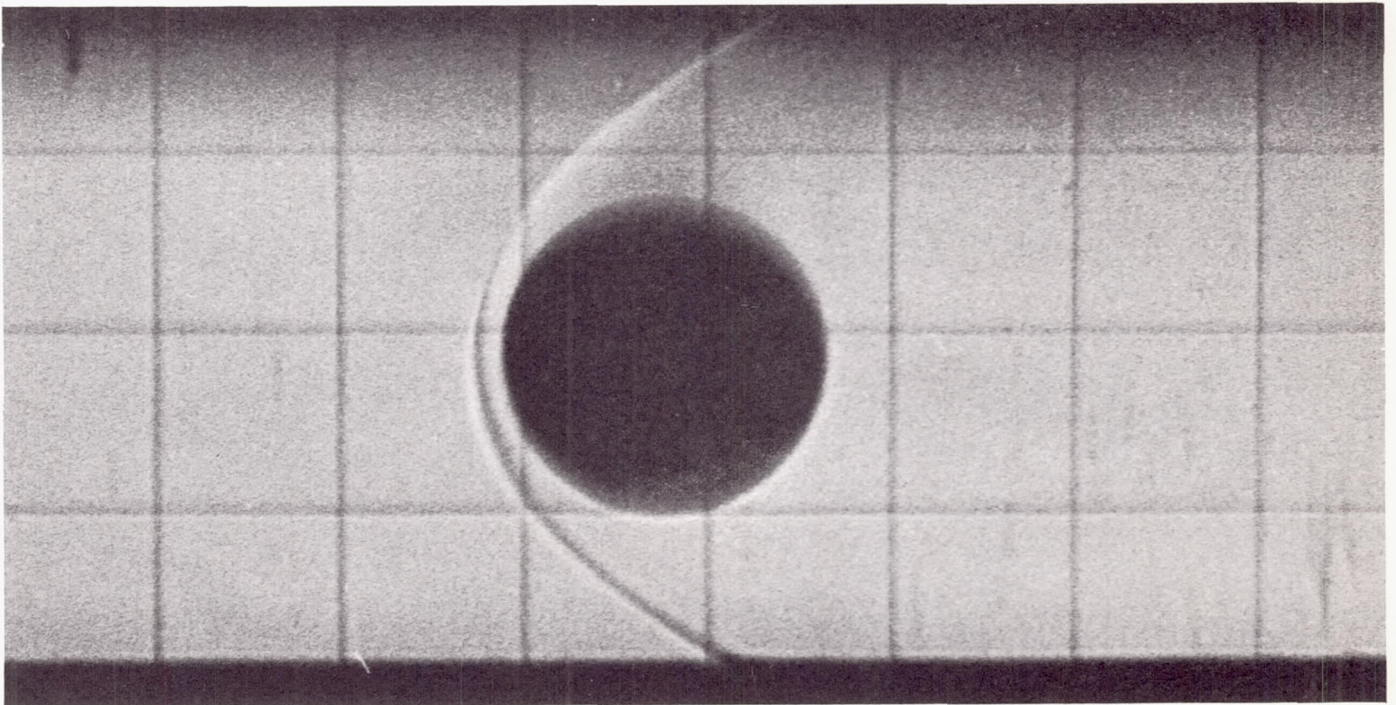
To obtain aerodynamic data such as drag and pitch-moment slope, high speed movies were made of the model motion in a plane parallel to the viewing-window surface. The lighting could be:

- (1) Front lighting.
- (2) Steady schlieren light but with the knife-edge cut-off removed (shadowgraph).

- (3) Backlighting with a ground-glass background which could be brilliantly illuminated in order to silhouette the model.

The front lighting technique seems to be less satisfactory than the other two methods. The backlight and the schlieren-light-source techniques give similar results except that with the backlight technique, more light could be applied, allowing the use of a slower, finer grain film. Parallax must be taken into consideration when using either the front- or back-lighted techniques, while this problem is eliminated by the use of the schlieren light source.

If it is desired to obtain model-motion data in orthogonal planes of motion, mirrors could be placed at 45-deg angles to the test section floor and ceiling, and parallel to the airflow. This would put all the data upon one roll



$M = 5$
 $P_t = 400 \text{ cm Hg}$
 $R_D = 1.3 \times 10^5$
 Model diam = $1\frac{1}{2}$ in.

35-mm Super Hypan film
 $f 5.6$; ASA 400
 4000 frames/sec

Direct picture of schlieren-system image. Knife-edge cut-off removed (shadowgraph). Grid spacing = 0.85 in.

Fig. 4. Example of 35-mm half-frame motion pictures taken at 4000 frames/sec

of motion picture film, each frame having the model attitude in each of the orthogonal planes. One problem is that care must be taken in order to obtain data without the model motion being affected by flow disturbances from these two 45 deg mirrors. This will limit the disturbance-free length of model travel at the lower Mach numbers.

At first, single-frame 16-mm film was used but later, half-frame 35-mm film at 4000 frames/sec was incorporated. The image on the 35-mm film appears to be

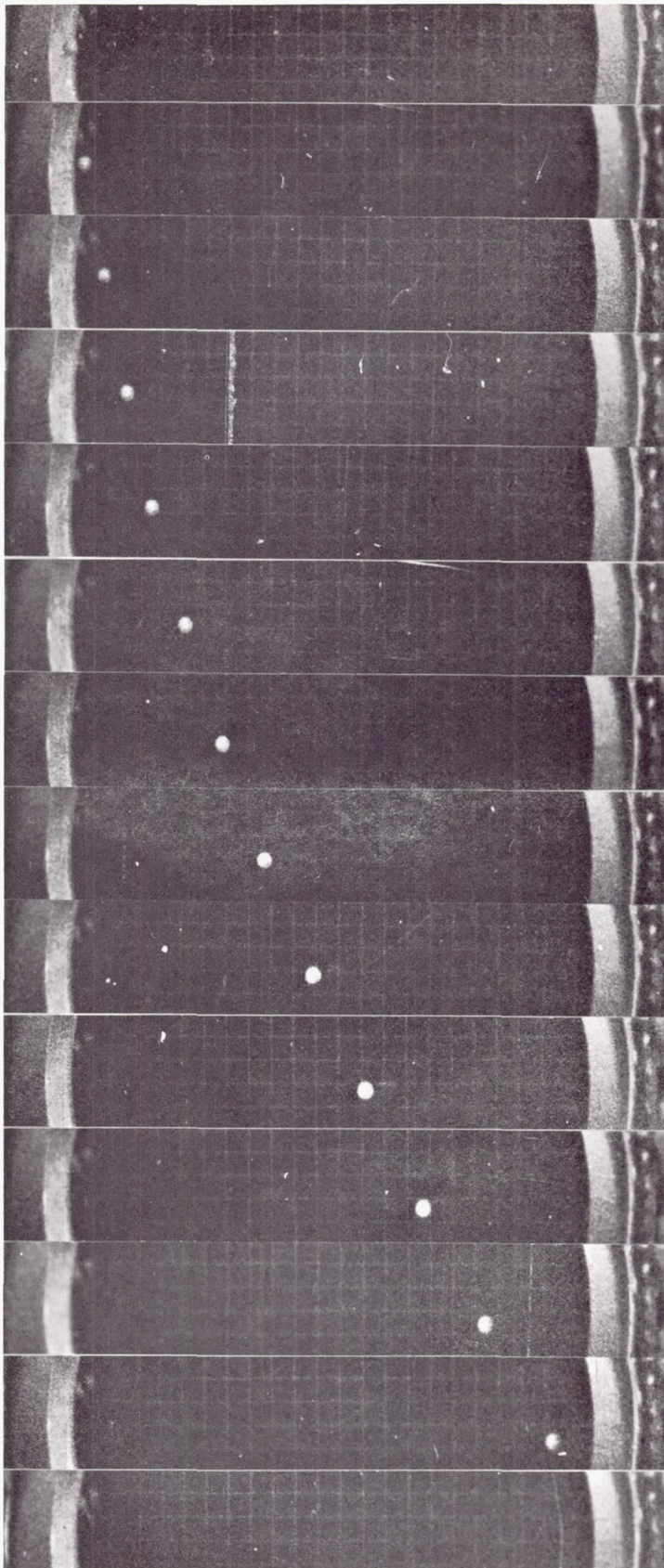
quite satisfactory for determining the model attitude. Initially the front-light technique was employed, but this gave way to taking pictures of the ground glass viewing screen of the normal schlieren system. This procedure was an improvement over the front lighting, even though the ground-glass grain limited the resolution. Finally, though, the ground glass was removed and the camera was focused directly upon the second image. This procedure yielded pictures substantially superior to any of the other motion-picture film examples included in this Report. An example of this technique appears in Fig. 4.

VI. SPHERE DRAG

At Mach 4 the drag of a 4.2 gram, 0.74-in. diam sphere was obtained from 16-mm high speed (4580 frames/sec) motion pictures using the front-lighted technique. Figure 5 shows the sphere motion across the viewing window. The model position history data are shown in Fig. 6 and the resulting velocity history data from which the acceleration was determined are shown in Fig. 7 along with the details of data reduction. Although the least satisfactory techniques (16-mm film with front light) were used for this condition, the resulting drag coefficient of

$C_D = 0.938$ at a Reynolds number (R_D) of 3.4×10^4 compares quite favorably (1½% difference) with the accepted ballistic range data of $C_D = 0.923$ (Refs. 4, 5).

Similar data have been obtained through the Mach number range of $M = 1\frac{1}{2}$ to 5 with high-speed (4000 frames/sec) 35-mm motion pictures of the schlieren system (no knife-edge cutoff) ground glass. This set of data is currently being reduced and will be presented in a subsequent report.



$M = 4$
 $P_t = 30 \text{ cm Hg}$
 $R_D = 3.4 \times 10^4$
Model diam = 0.74 in.
16-mm Tri-X film
f 2.8; ASA 320
4580 frames/sec
Model weight = 4.2 g
Front-lighted technique. Every 25th frame is shown;
0.00546 sec between each printed frame.
Grid spacing = 1 in.

Fig. 5. Pictures showing travel of sphere model across viewing window

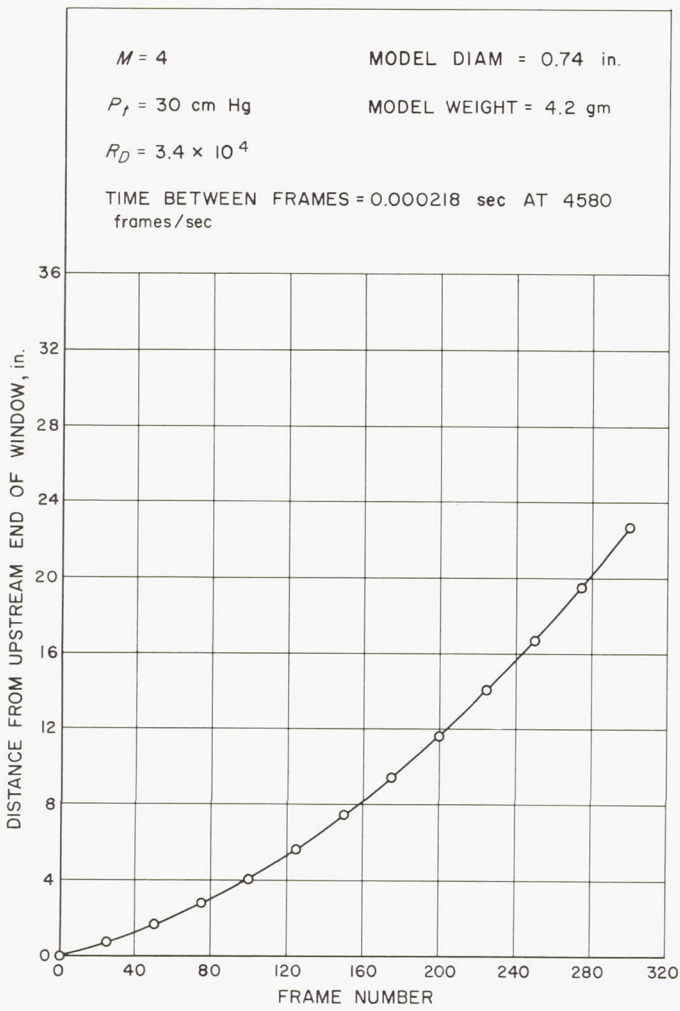


Fig. 6. Model-position history of free-flight sphere

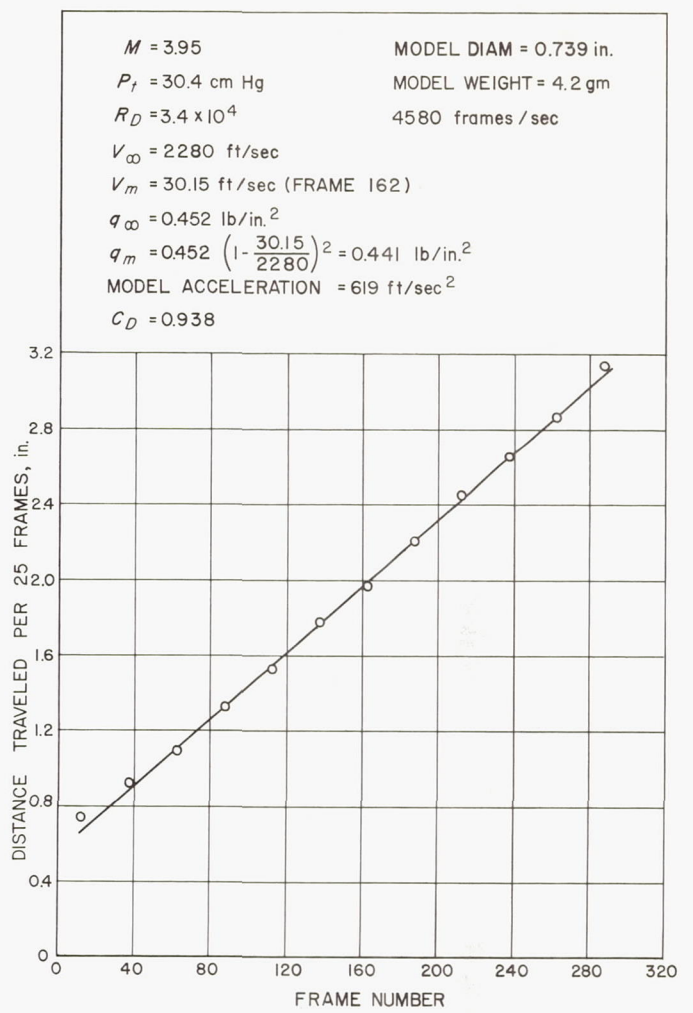


Fig. 7. Velocity history of free-flight sphere

VII. FREE-FLIGHT SPHERE WAKES

In order to obtain high-resolution schlieren data of a free-flight sphere wake, a timer was hooked up to the spark system (3- μ sec duration) and a proper delay was initiated by the parting of the supporting vertical wire. Examples of such pictures are shown in Fig. 8 for $M = 3$

and 4. Additional data have been obtained through the Mach number range from $M = 1\frac{1}{2}$ to 5 and a report on these data is being published. The spark shadowgraph of a free-flight sphere at $M = 4$ shown in Fig. 8 does not have the wake detail of the spark schlieren pictures.

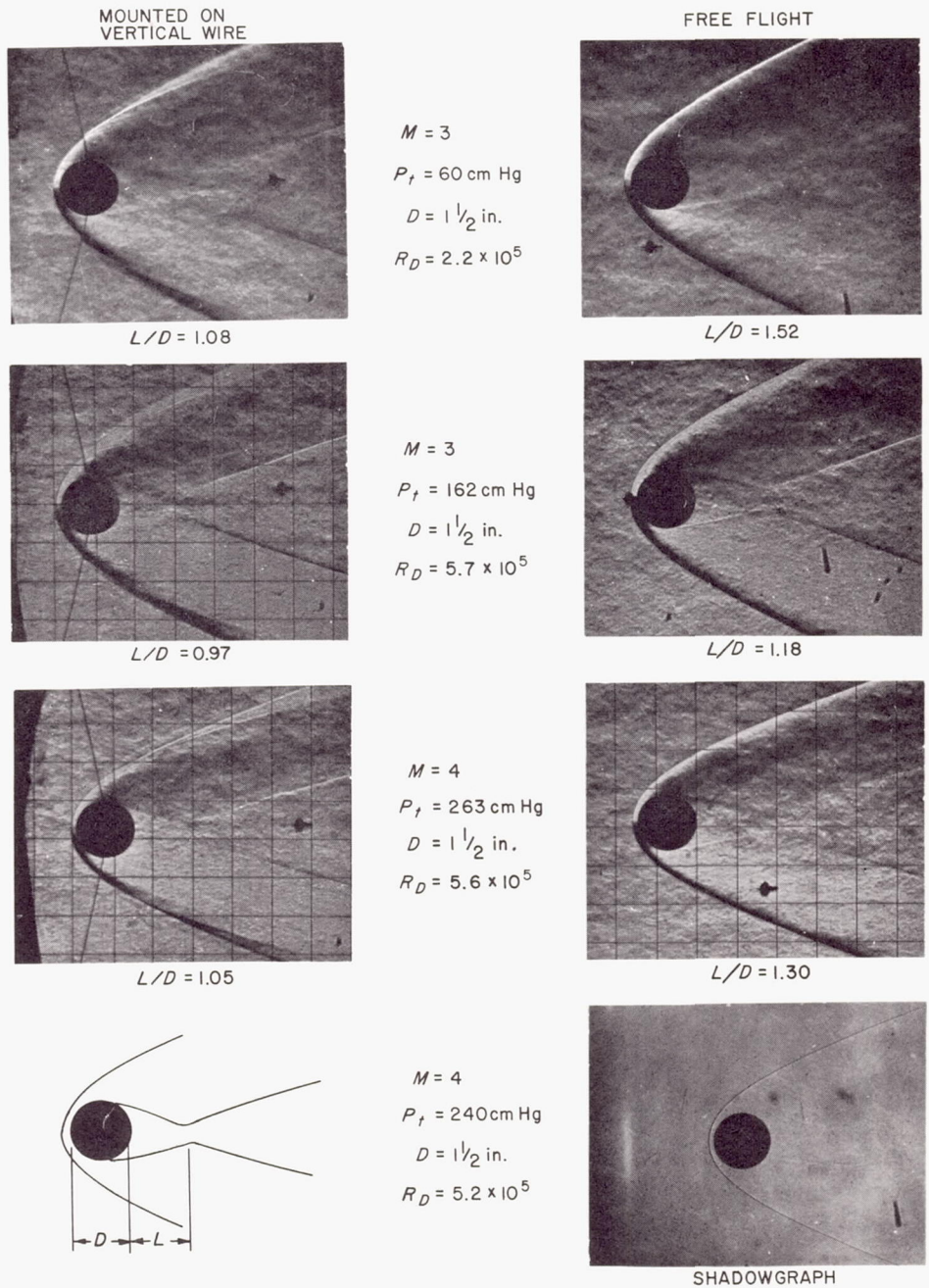


Fig. 8. Spark schlieren pictures of sphere wakes

VIII. EFFECT OF VERTICAL WIRE SUPPORT ON SPHERE WAKES

A consequence of the acquisition of the free-flight sphere-wake spark schlieren pictures was the comparison of the free-flight wakes with those of the 1½-in. diam spheres while supported on 0.020-in. diam vertical wires. The wire decreased the length of the separation region behind the sphere by a considerable amount. The effect of the wire support is shown in Fig. 8 along with sample free-flight sphere-wake spark schlieren pictures. At $M = 3$ a fairly extensive investigation was made of the effects of various wire diameters and orientations (vertical or horizontal or both) at several Reynolds numbers. These

effects will be included in the free-flight sphere-wake report now being published.

The result of these interference investigations is that these relatively small wire supports do have a significant effect upon the sphere wake. The usual approach of supporting models on wires in order to obtain data for models having no support interference is subject to criticism—at least it is a questionable technique for short, blunt shapes such as spheres. Perhaps the wires may not have quite so severe an effect on the wakes of longer, less blunt shapes.

IX. AERODYNAMIC-SHAPE FREE-FLIGHT DATA

Several 10 deg half-angle cone models, each one blunted with an $r/D = 0.423$ spherical segment, and having a total length of $l = 0.825D$, were made in order to check out the simplified free-flight testing technique in a conventional wind tunnel (see Fig. 9). These 1-in. diam models were cast of 2 lb/ft³ polyurethane foam and weighed approximately 1 gram. (It should be noted that the foam density at the outer surface was about 8 lb/ft³ while that at the center was about 4 lb/ft³, resulting in an average foam density of about 6 lb/ft³.) The models were drilled from the base and a 0.45-in. diam spherical lead core (about 8½ grams) was inserted in such a manner as to put the model cg at $0.424D$ from the nose. A photograph of this type of model is shown in Fig. 2.

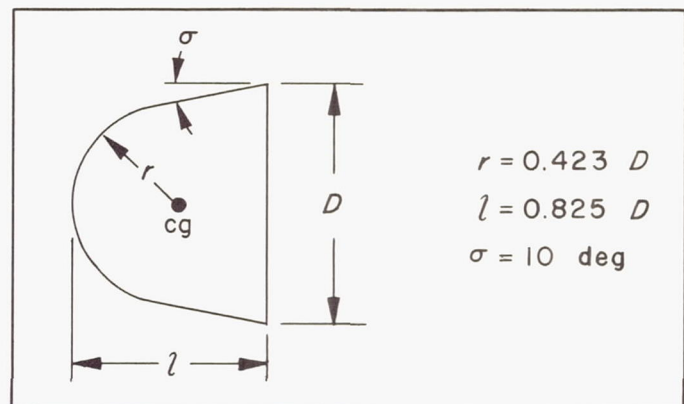


Fig. 9. Aerodynamic-shape model dimensions

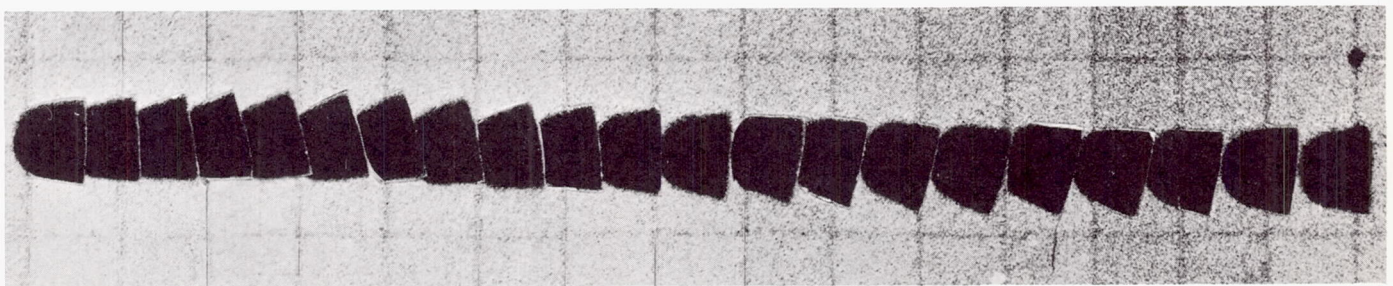
For the model supported on a horizontal string a run was made at $M = 4$, supply pressure of 80 cm Hg, and initial model attitude of 17 deg angle of attack in the plane parallel to the viewing window surface. A sample of the resulting model motion is shown in Fig. 10. As can be seen by the relative flatness of the model base, the oscillatory motion is largely confined to the initial plane of angular displacement. The motion was recorded on 35-mm film at 4390 frames/sec. The image is somewhat fuzzy as the camera was focused upon the schlieren viewing screen and the grain of the ground glass was considerably coarser than the film grain. Subsequent pictures taken with the ground glass removed are of substantially improved quality. The model motion deduced from data similar to that in Fig. 10 is shown in Fig. 11. Even with the problem of the ground glass grain, the resolution was good enough to obtain a fairly good history of the oscillatory motion. The distance-traveled data do not require extremely high picture quality in order to be of high accuracy.

From the oscillatory data the frequency of oscillation comes out to be 45 cps. Using an estimated (calculated) model moment of inertia and center of gravity location (they were not experimentally measured) the pitch moment coefficient slope was determined to be $-0.147/\text{rad}$. The equivalent sting-supported static stability test value is $-0.127/\text{rad}$ for an angle of attack region of $0 \text{ deg} < \alpha < 16 \text{ deg}$. Using data reduction techniques similar to those shown in the sphere drag discussion, the effective drag coefficient of this shape as it oscillated between $\pm 16 \text{ deg}$ came out to be $C_D = 0.734$. From the sting-mounted force test the average drag coefficient for this

oscillatory motion is calculated to be $C_D = 0.743$. A summary of the drag data reduction is shown in Fig. 12.

This model shape was released at $M = 3$ (162 cm Hg supply pressure) using the weathervane technique from a vertical wire. The model oscillation was essentially in the plane perpendicular to the viewing window surface. The amplitude of oscillation was approximately $\pm 40 \text{ deg}$. High-speed (3910 frames/sec) 35-mm motion pictures were taken of the schlieren system viewing ground glass for two conditions: (a) with the knife-edge cut-off in place in order to show the flow field using the normal schlieren technique; and (b) with the knife-edge removed in order to give a light background so that the model is silhouetted. A sample half-cycle of these data is shown in Fig. 13. Note should be taken of how the wake shape varies with angle of attack. For purposes of comparison a spark shadowgraph of this model is shown in Fig. 14. ($M = 4$ but at the considerably lower supply pressure of 60 cm Hg).

A total of 105 frames of data recorded the model in flight while it went through $2\frac{1}{2}$ complete cycles of oscillation. It is quite easy to accurately determine both the pitch-moment slope and the drag of the models, but the reduced data lack indication of the exact amplitude of oscillation. An initial angle of about 40 deg was set prior to model release, and the data reduction indicates that it is quite likely that this was the region of the oscillatory amplitude during the flight. It is not possible to estimate the model oscillation amplitude to within 5 deg from the pictures shown in Fig. 13.



$M = 4$	35-mm Super Hypan film
$P_t = 80 \text{ cm Hg}$	f 4.0; ASA 500
$R_D = 1.2 \times 10^5$	4390 frames/sec
Model diam = 1 in.	Model weight = 9.5 g

Picture of image on ground-glass viewing screen. Knife-edge cut-off removed (shadowgraph). Amplitude of oscillation is about $\pm 16 \text{ deg}$ in plane parallel to viewing window. Every 5th frame is shown; 0.00114 sec between each model position.

Fig. 10. Composite picture of aerodynamic shape in flight

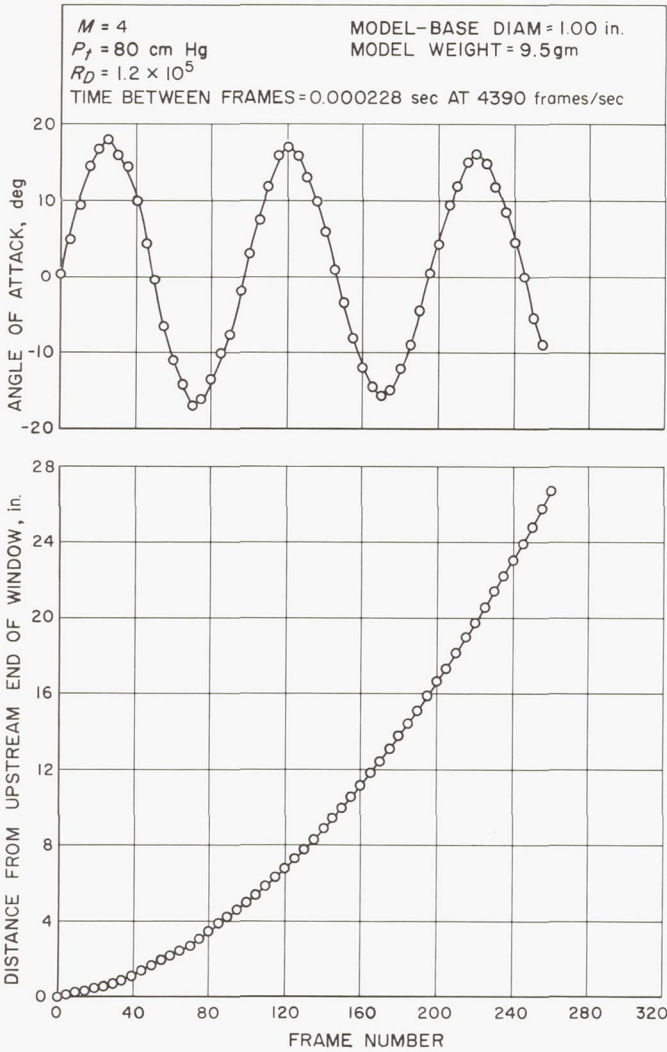


Fig. 11. Model-position history of aerodynamic shape

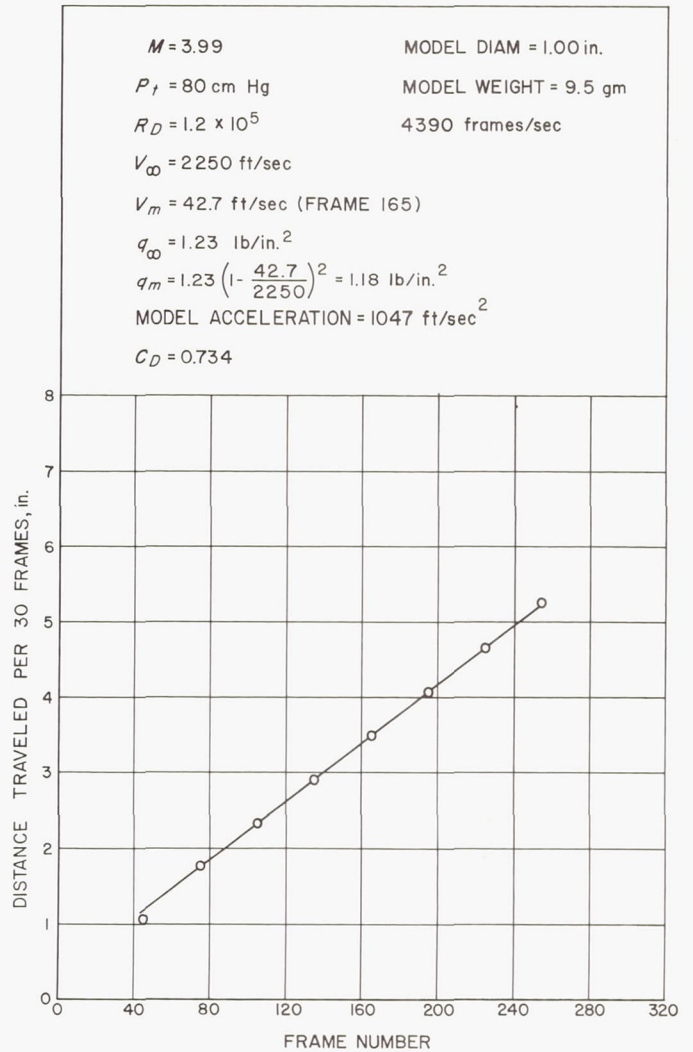
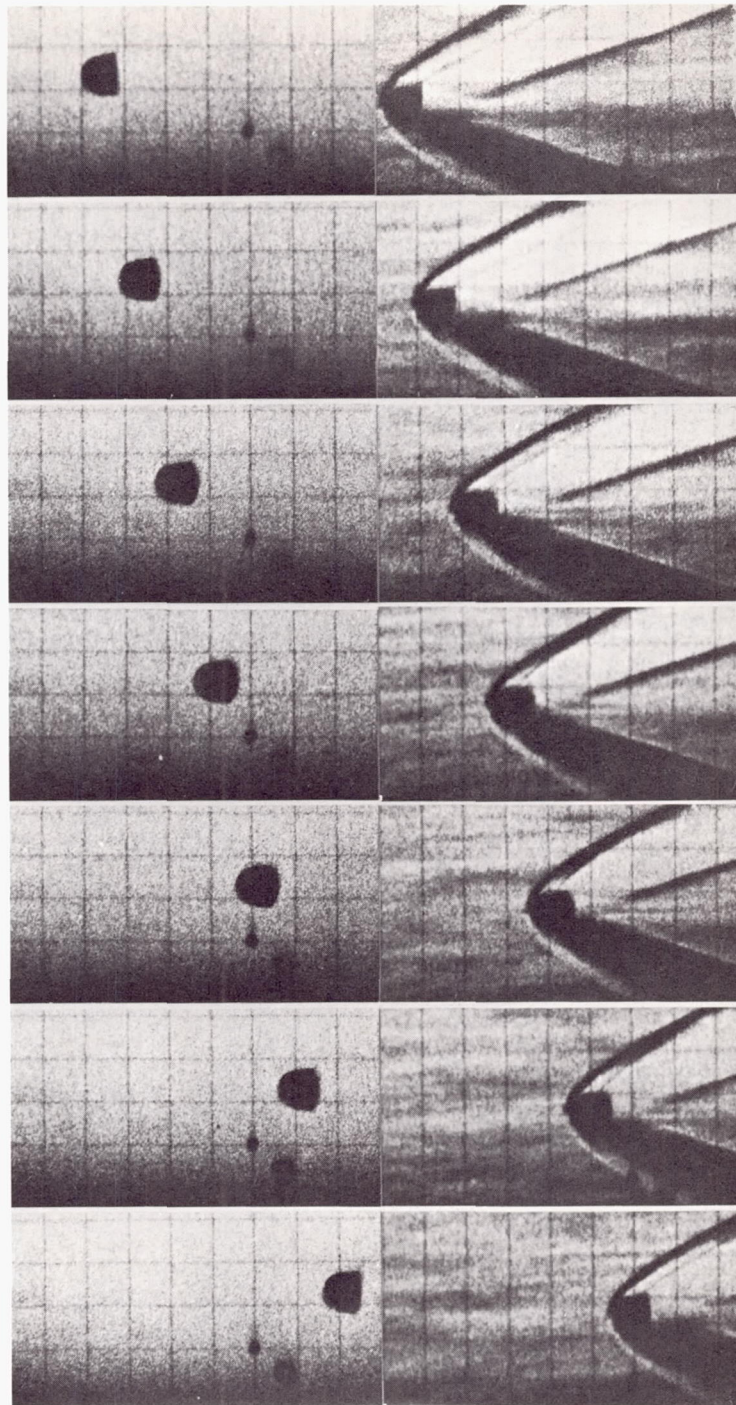


Fig. 12. Velocity history of aerodynamic-shape model

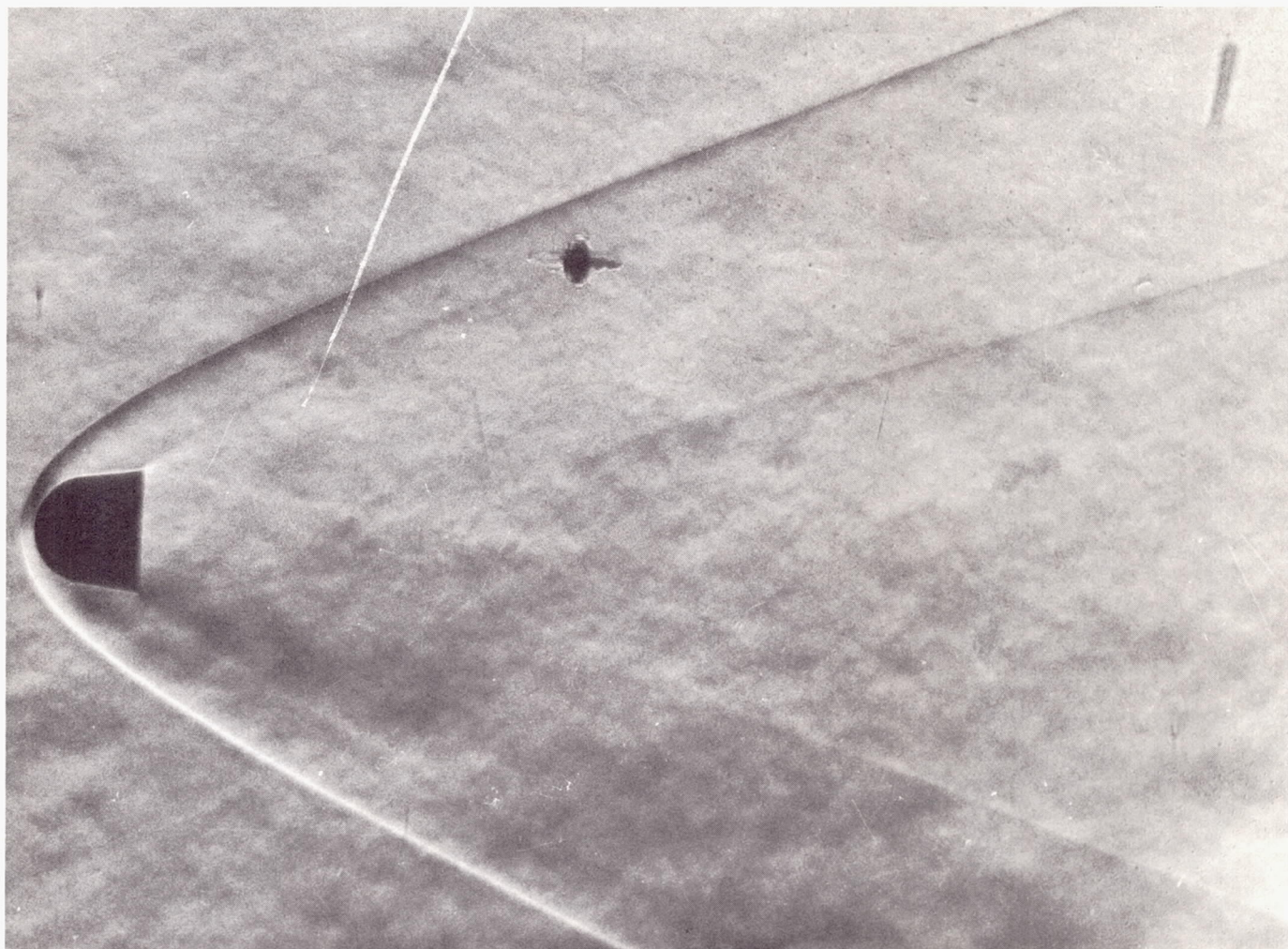


$M = 3$
 $P_t = 162 \text{ cm Hg}$
 $R_D = 3.8 \times 10^5$
 Model diams = 1 in.

35-mm Super Hypan film
 $f 4.0$; ASA 500
 3910 frames/sec
 Model weights = 9.5 g

Picture of image on ground-glass viewing screen. Amplitude of oscillation is about ± 40 deg in plane normal to viewing window. Every 3rd frame is shown; 0.00077 sec between each model position. Grid lines are on 1-in. centers.

Fig. 13. Composite pictures of aerodynamic shapes in flight



$M = 3$
 $P_t = 60 \text{ cm Hg}$
 $R_D = 1.5 \times 10^5$

Model diam = 1 in.
Angle of attack ≈ 0 deg

Fig. 14. Free-flight spark schlieren picture of aerodynamic-shape model

X. SUMMARY OF SOME ADVANTAGES OF FREE-FLIGHT TESTING IN A WIND TUNNEL

The descriptions of the various free-flight tests presented in this Report serve to document the feasibility of this testing technique. A great deal of work remains to be done to make such testing operational. It would be informative to list various types of tests that could benefit from the use of the free-flight technique in a conventional wind tunnel in contrast to the usual sting mounted tests.

A. Drag

The presence of a sting support affects the model base pressure. At low Mach numbers the base pressure can be a major portion of the total drag, especially for long, slender models. Thus it becomes virtually impossible to measure the total drag of certain models accurately (say within $\pm 2\%$) when they are supported on a sting as the sting can considerably alter the base pressure. For purposes of illustration, Table 1 indicates the importance of the base pressure drag on a 20-deg half-angle cone. For simplification it was assumed that the base pressure is one-half of freestream pressure. This is not exactly the actual case, but is probably within a factor of two of being the usual condition, hence is certainly an adequate assumption to point out the importance of an error in the base pressure when correct total drag is a test requirement.

Table 1. Analytical estimate of cone drag
(20-deg half angle)

M	C_{D_P}	C_{D_B}	C_{D_T}	C_{D_B}/C_{D_T}
1 1/4	0.489	0.457	0.946	0.92
2	0.325	0.179	0.504	0.36
5	0.259	0.029	0.288	0.10
10	0.250	0.007	0.257	0.03

It is readily apparent that a 10% error in the base pressure (which is certainly a real possibility because of sting interference) can cause a significant error in the total drag at the lower Mach numbers. The base pressure effect on total drag is considerably more serious and extends further into the higher Mach number region as the cone becomes more slender.

Determining the drag on a model in a wind tunnel at very low Reynolds numbers is a difficult problem. The minimum model size is determined by the balance size, and the balance loads are in turn controlled to some

degree by the starting loads (in many cases wind tunnels can operate at far lower pressures than those at which flow can be established). Also, small sensitive drag balances are difficult to build and to keep operational. These difficult, but not necessarily insurmountable, problems can be avoided by the use of the free-flight technique. For example, models as small as 0.1-in. in diam can be tested at $M = 5$ in the JPL 20-in. SWT at the minimum operational Reynolds number per inch of 2.5×10^4 (supply pressure = 25 cm Hg) giving a model Reynolds number (R_D) of 2500. Perhaps the use of front-lighted techniques would permit the use of even smaller models for drag measurements.

The comments made about model size and the detrimental effects of sting and support interference on drag data also apply to the following discussions on pitch moment and pitch damping data.

B. Base Pressure

Should it be desirable to determine the true base pressure on a model under wind tunnel conditions, the optimum approach would be to have a model with no support. The usual wind tunnel technique is to support the model with wires or a winged side-support or use a series of decreasing sizes of stings and extrapolate the data to zero sting diameter. As results of these preliminary free-flight investigations indicate the large effect of wire supports on the wake shape, hence a corresponding effect on the base pressure level, it appears that the use of wires or side support may not be adequate for obtaining the true base pressure. It certainly would be desirable to obtain the true supportless base pressure in order to determine the validity of the method which involves using decreasing sizes of stings, and extrapolating the data to zero sting diameter. In the free-flight wind tunnel technique, the maximum acceleration experienced by the model prior to and during the useful trajectory is usually below $10^2 g$. To put telemetry equipment in such models is certainly a minor problem relative to what is done at a ballistic range where the launch accelerations are above $10^5 g$.

C. Wake Shape

In many cases it is desirable to know the proper wake shape of a particular model. Force and moment data

obtained in a wind tunnel for sting-supported models are definitely a function of the wake shape, especially so at the lower Mach numbers ($M < 2$). The determination of the undisturbed wake shape can easily be obtained by the described free-flight technique. The knowledge of the proper wake shape would aid in the evaluation of such force and moment data. In fact, the wake shape of a sting-supported model can be altered by applying suction on the sting and perhaps can be used to duplicate the free-flight wake shape of a sting-supported model for a force-moment test.

D. Pitch Moment

It has been shown that it is a relatively simple matter to determine the frequency of a model's oscillation during its trajectory. This information (in conjunction with the model mass characteristics) is sufficient for determining the effective pitch-moment slope. As long as the oscillatory model motion lies in the plane crosswise to the viewing direction, the amplitude of oscillation can be obtained in order to give meaning to the pitch moment. Of course the use of a pair of 45 deg mirrors would guarantee complete knowledge of the model attitude under nonideal conditions.

As models need not withstand high accelerations, they can be easily constructed to put the center of gravity well toward the model nose. This is an extremely difficult achievement for ballistic range models.

E. Pitch Damping

It is known that at low Mach numbers ($M < 2$) the base geometry of a model can affect the pitch damping. From this it can be inferred that a sting also will affect the pitch damping. Hence it is desirable to use free-flight techniques to obtain this information. Sometimes the basic design of certain configurations virtually prohibits captive (supported) means of pitch-damping testing. An example of this is the *Apollo* abort configuration (re-entry capsule and tower with rocket) where the center of gravity could lie within the fine skeletal framework of the tower. The pitch damping of this type of model can be adequately measured by a free-flight technique if the damping is not too small.

It is not yet clear to what degree of accuracy pitch damping can be obtained. No runs have yet been made of oscillating aerodynamic shapes using the optimum photographic techniques that have been developed during these feasibility studies. Until such data are obtained and the angle of attack histories are measured, it will not be possible to reach definite conclusions on the use of this wind tunnel free-flight technique for the determination of pitch damping. However, the results to date are very encouraging, and coupled with the equivalent of 100 to 300 viewing stations, it appears to be possible to obtain useful (and repeatable) pitch damping data from wind tunnel free-flight testing.

XI. ADDITIONAL COMMENTS

This free-flight testing technique in a conventional wind tunnel is being presented simply as a complement to those methods now being used in wind tunnels and in ballistic ranges. Like any testing procedure, it has advantages as well as disadvantages. For example, the model environment in a ballistic range is real gas while in a conventional wind tunnel the gas is nearly ideal. Certainly at the higher Mach numbers the aerodynamic forces on a model caused by a real gas can differ from those caused by an ideal gas. The specific heat ratio of the air in the usual supersonic wind tunnel is very near the ideal 1.40. At a pressure of $\frac{1}{10}$ atmosphere, the specific heat ratio of air will drop to 1.35 from 1.40 as the temperature is raised from 546°R to 1512°R . Probably for most general testing, this is not enough of a variation in specific heats to affect the aerodynamic force and moment data. (It should be pointed out that aerodynamic tests are continually being carried out at Mach numbers up to 20 in gases where the specific heat ratio is far different from real gas conditions at the respective Mach numbers. Both flight and ballistic range data validate this questionable testing technique.) The point being made here is that perhaps ballistic range testing has no major advantages (except for high R_D) over free-flight testing in a wind tunnel up to $M = 4$ as the specific heat ratio of the air over a blunt model is about 1.34 in a range, as against 1.40 in an unheated supersonic wind tunnel. Actually, in

the JPL hypersonic wind tunnel, the air can be heated to 1700°R which will duplicate actual high altitude flight conditions of temperature and pressure at $M = 4$.

Another very important feature in ballistic range testing occurs at the higher Mach numbers ($M > 5$) where the model wall temperature is cool relative to the air temperature around the model, a condition which exists in actual flight. This is a very important feature for models having regions of adverse pressure gradients (such as cylindrical models having flared afterbodies) where the ratio of model wall temperature to the freestream air temperature can affect the flow field about the model. An uncooled flared model when tested in a wind tunnel at the higher Mach numbers ($M > 5$) may have separated flow ahead of the flare. This region of separation will decrease as the model wall is cooled, and can become quite small at liquid nitrogen temperatures (Refs. 6, 7). It should be possible to cool the model prior to release in wind tunnel free-flight testing in order to control the model wall temperature. Furthermore this wall temperature could be varied in order to determine the effects of wall temperature on the model aerodynamic force and moment data. The use of this cooling technique prior to model release further helps to make this wind tunnel free-flight testing technique approach actual flight conditions.

XII. FUTURE WORK

Rather than go into a lengthy discussion on the efforts of free-flight testing that are being contemplated, a brief outline of the planned work at JPL is presented here. Even though this list is far from complete, it does serve to indicate the large amount of work yet to be done. Concurrent with the further development of free-flight testing in the JPL wind tunnels (both the supersonic $\{1\frac{1}{4} < M < 5\frac{1}{2}\}$ and the hypersonic $\{4 < M < 11\}$), routine test work will be done which utilizes the advantages of free-flight testing over the conventional sting-support testing in a wind tunnel.

A. Model Construction

1. Thin metal coating over light-weight foam
2. Bi-material: heavy metal for nose; light material for remainder
3. Ultra light-weight and very small models

B. Model Support and Release Techniques

1. Air gun on tunnel centerline to propel models into viewing area—will give double the amount of data of wire supported system
2. Exploding (by electrical power) wire technique—would permit use of
 - (a) Horizontal wire instead of string
 - (b) Multi-wire support

3. Use of single vertical wire to support models at initial angles of attack with less chance of model instability while on wire

C. Greater Variety of Data

1. Cool model walls with
 - (a) Liquid nitrogen (-300°F wall temperature)
 - (b) Gaseous nitrogen (0°F wall temperature)
2. Telemetered base pressure
3. Improve image on film
 - (a) Finer grain film
 - (b) Greater amount of light
 - (c) Multiple spark techniques
4. Improve flow visualization techniques

D. Data Reduction

1. Measurement of the various model mass characteristics
 - (a) Weight
 - (b) Center of gravity
 - (c) Moment of inertia
 - (d) Dimensions (especially for very small models)
2. Film reading
3. Ballistic range data reduction procedures

XIII. CONCLUSIONS

Although the data presented in this Report are preliminary and are not of the high quality which can be achieved by using the recommended techniques, the results of this simplified free-flight testing in a conventional wind tunnel are very encouraging. Time and effort were not expended to determine the many data reduction constants accurately (such as model weight, moment of inertia, center of gravity, etc.), but rather to develop the basic fundamentals of this type of testing. Inaccuracies in the data reduction constants affect only the level of the final data, but not the sensitivity. The minor scatter in the model acceleration data and the ease of determining the oscillation frequency and amplitude history serve to indicate the feasibility of this testing technique. As an example, acceleration data obtained simultaneously by both the front-lighted and the shadowgraph techniques

of a single-sphere drag run were in agreement to within 1% of each other.

More precise reduction techniques (such as used in ballistic range work) coupled with the analysis of each of the several hundred frames of data per flight (rather than just reading every third or fifth frame with a ruler and a protractor as was done for this presentation) should give final data of consistently high quality. This report has shown that it is quite practical to obtain a wide variety of highly accurate aerodynamic data on models with no support interference by free-flight testing in a wind tunnel; but that a great deal of work remains to be done in order to fully explore the many possibilities in order to assess the advantages and limitations of this testing procedure and to make it fully operational.

NOMENCLATURE

a	model acceleration
A	model reference area
C_D	model drag coefficient = drag/ qA
C_{D_B}	drag coefficient due to base pressure
C_{D_P}	drag coefficient due to pressure on conical surface
C_{D_T}	total drag coefficient
C_{m_α}	model pitch-moment slope coefficient = M_α/qAd
$C_{m_q} + C_{m_{\dot{\alpha}}}$	pitch damping coefficient
d	model reference length
f	oscillation frequency
g	acceleration due to gravity
HWT	hypersonic wind tunnel
I	total moment of inertia of spherical model about its center of gravity
m	mass of model
M	Mach number
M_D	pitch damping
M_α	pitch moment slope/radian
P_t	supply pressure
q	dynamic pressure, $\frac{1}{2}\rho V^2$
q_m	dynamic pressure on model
q_∞	tunnel freestream dynamic pressure
r_c	radius of core of spherical model
r_s	radius of outer shape of spherical model
R_D	Reynolds number
SWT	supersonic wind tunnel
t	time
V_m	model velocity
V_∞	tunnel freestream velocity
W	weight of model = mg
α	angle of attack
α_t	amplitude of oscillation at time t
α_0	amplitude of oscillation at $t = 0$
ρ	air density

REFERENCES

1. Harris, C. J. and Warren, W. R., of the General Electric Space Sciences Laboratory, Missile and Space Vehicle Department, King of Prussia, Pennsylvania, "An Experimental Study of the Aerodynamic Characteristics of Finned Re-Entry Vehicles," paper presented at the 1961 Air Force-Aerospace Corporation Symposium on Ballistic Missile and Aerospace Technology, University of Southern California, Los Angeles, California.
2. Gates, D. F. and Bixler, D. N., *The Measurement of Aerodynamic Forces and Moments in the NOL 4-in. Hypersonic Shock Tunnel No. 3*, NOLTR 6-100, United States Naval Ordnance Laboratory, White Oak, Maryland, September, 1961.
3. Lukasiewicz, J., Jackson, R., and van der Bliet, J. A., of the von Karman Gas Dynamics Facility, Arnold Engineering Development Center, Tullahoma, Tennessee, and Harris, W. G. and Miller, R. M., of Boeing Airplane Company, Seattle, "Development of Capacitance and Inductance Driven Hotshot Tunnels," paper presented at the 1960 Hypervelocity Technique Symposium, University of Denver, Denver, Colorado.
4. Charters, A. C. and Thomas, R. N., "The Aerodynamic Performance of Small Spheres from Subsonic to High Supersonic Velocities," *Journal of the Aeronautical Sciences*, Vol. 12, No. 4, October, 1945, pp. 468-76.
5. Hodges, A. J., "The Drag Coefficient of Very High Velocity Spheres," *Journal of the Aeronautical Sciences*, Vol. 24, No. 10, October, 1957, pp. 755-58.
6. Schaefer, J. W. and Ferguson, H., of the National Aeronautics and Space Administration Lewis Research Center, "Investigation of Separation and Associated Heat Transfer and Pressure Distribution on Cone-Cylinder-Flare Configurations at Mach Five," *American Rocket Society Journal*, Vol. 32, No. 5, May, 1962, pp. 762-70.
7. Minich, J. J., "Tunnel Development Test 21-207-Flow Separation at Hypersonic Velocities," *Jet Propulsion Laboratory Space Program Summary 37-16*, Vol. IV, June-July, 1962, Jet Propulsion Laboratory, Pasadena, California.